Encapsulation of C_{60} fullerenes into single-walled carbon nanotubes: Fundamental mechanical principles and conventional applied mathematical modeling

Duangkamon Baowan, Ngamta Thamwattana, and James M. Hill
Nanomechanics Group, School of Mathematics and Applied Statistics, University of Wollongong, New South Wales 2522, Australia
(Received 30 April 2007; revised manuscript received 1 August 2007; published 15 October 2007)

A well-known self-assembled hybrid carbon nanostructure is a nanopeapod which may be regarded as the prototype nanocarrier for drug delivery. While the investigation of the packing of C_{60} molecules inside a carbon nanotube is usually achieved through either experimentation or large scale computation, this paper adopts elementary mechanical principles and classical applied mathematical modeling techniques to formulate explicit analytical criteria and ideal model behavior for such encapsulation. In particular, we employ the Lennard-Jones potential and the continuum approximation to determine three encapsulation mechanisms for a C_{60} fullerene entering a tube: (i) through the tube open end (head-on), (ii) around the edge of the tube open end, and (iii) through a defect opening on the tube wall. These three encapsulation mechanisms are undertaken for each of the three specific carbon nanotubes (10,10), (16,16), and (20,20). We assume that all configurations are in vacuum and the C_{60} fullerene is initially at rest. Double integrals are performed to determine the energy of the system and analytical expressions are obtained in terms of hypergeometric functions. Our results suggest that the C_{60} fullerene is most likely to be encapsulated by head-on through the open tube end and that encapsulation around the tube edge is least likely to occur because of the large van der Waals energy barriers which exist at the tube ends.

DOI: 10.1103/PhysRevB.76.155411 PACS number(s): 61.46.Fg, 61.48.+c, 81.05.Tp, 34.20.Gj

I. INTRODUCTION

Carbon nanostructures such as carbon nanotubes and C_{60} fullerenes have received considerable attention for their potential applications in many future nanoscale devices. This is because of their underlying unique mechanical properties arising from the van der Waals interaction force and their electronic properties arising from the large surface to volume ratio.[1,2] The combination of a single-walled carbon nanotube and a C_{60} fullerene chain, a so-called nanopeapod, also embodies such properties and is a new hybrid nanostructure, which might also be exploited as a component in nanoscale devices. Nanopeapods were originally observed in 1998 by Smith *et al.*[3] and later synthesized by Smith and Luzzi,[4] who employ high-resolution transmission electron microscopy to show the self-assembly of the hybrid structures. In particular, nanopeapods may be regarded as the prototype nanocarrier for drug delivery, where the carbon nanotube can be thought of as the nanocontainer and the C_{60} molecule chain can be considered as the drug molecule.[5]

Several studies have proposed the actual assembly of nanopeapods by utilizing either experimentation or computer simulation. Qian *et al.*[6] employ molecular dynamics studies and suggest that the (9,9) and (10,10) single-walled carbon nanotubes will accept a C_{60} molecule from rest but this behavior will not occur for the (8,8) carbon nanotube. From the study of the energetics and electronic structures of nanopeapods, Okada *et al.*[7] propose that the smallest radius of a nanotube which can encapsulate a C_{60} molecule is approximately 6.4 Å, which is approximately the radius of a (10,10) carbon nanotube. This result compares well with Hodak and Girifalco[8] and Cox *et al.*,[9] but conflicts with Qian *et al.*[6] who show that the fullerene can be accepted into a (9,9) nanotube which has a radius of 6.102 Å. Moreover, from Okada *et al.*,[7] Hodak and Girifalco,[8] and others,[5,10–13] it is confirmed that the encapsulation energy of nanopeapods depends only on the tube radius, and that it is independent of the tube chirality.[12]

There are three possible scenarios for C_{60} molecules to become encapsulated into a carbon nanotube and form a nanopeapod. The first such scenario is that the C_{60} molecule is sucked in through the tube open end when the C_{60} fullerene is originally located outside the tube but situated on the tube axis, and in a head-on configuration.[14] The encapsulation of the C_{60} fullerene around the edge of the tube is a second possible scenario and the final possible scenario is the absorption of the C_{60} fullerene through a large defect opening on the tube wall. These three encapsulation scenarios are investigated by Berber *et al.*,[15] who use the electronic Hamiltonian method, and Ulbricht and Hertel[14] and Ulbricht *et al.*,[16] who utilize molecular dynamics calculations based on the Lennard-Jones potential function. Berber *et al.*[15] suggest that the encapsulation of the C_{60} molecule is most likely to occur at a defect opening of the tube wall. In contrast, Ulbricht and Hertel[14] and Ulbricht *et al.*[16] propose that the C_{60} fullerene is most likely to be encapsulated by head-on at the tube ends. Moreover, they find that although encapsulation around a tube edge and absorption at a defect opening can occur, these outcomes are less likely.

To the authors' knowledge, very little work has been undertaken on the mathematical modeling to describe the encapsulation behavior of nanopeapods. The aim of this paper is to utilize fundamental mechanical principles and conventional applied mathematical modeling to determine the energy behavior for these three encapsulation scenarios of the C_{60} fullerene. In addition, the Lennard-Jones potential function for nonbonded atoms and the continuum approximation, which assumes that the interatomic interactions can be modeled by smearing the atoms uniformly across the surfaces, are employed to determine the van der Waals energy for the

 ©2007 The American Physical Society

C_{60} fullerene encapsulated into a carbon nanotube. In particular, we investigate (10,10), (16,16), and (20,20) carbon nanotubes whose radii are in the range 6.27–13.57 Å following Hodak and Girifalco[17] who determine fullerene peapod patterns. Carbon nanotubes with radii smaller than that of a (10,10) nanotube are not studied here, since it has already been shown that a C_{60} fullerene will not be sucked into such tubes (see, for example, Cox *et al.*[9]). Generally, for (n,m) carbon nanotubes, where n and m are integers, the corresponding radius, denoted here as b, is determined from

$$b = \sigma\sqrt{3(n^2+nm+m^2)}/2\pi, \tag{1}$$

where σ is the C-C bond length and throughout this paper σ is taken to be 1.42 Å. We comment that by adopting the continuum approximation, the chirality effect of a carbon nanotube is not taken into account, and the use of (n,m) in this paper therefore refers only to a representative of the tube size given by Eq. (1). In all cases, a vacuum environment and an isothermal mechanical system are assumed, and the C_{60} fullerene is assumed initially to be at rest. The Lennard-Jones potential function is described in the following section. In sections III and IV, the investigations for the C_{60} molecule encapsulated (i) head-on at the tube end and (ii) around the tube edge are examined. Section V presents the absorption of the C_{60} fullerene through a defect opening on the tube wall. Finally, a summary is presented in Sec. VI.

II. POTENTIAL ENERGY FUNCTION

The Lennard-Jones potential function for nonbonded molecules and the continuum approximation are employed here to determine the energy of the system. The total interaction energy for two nonbonded molecules is obtained by performing two double integrals for the two molecules and is given by

$$E = \eta_1\eta_2\int\int_R\left(-\frac{A}{r^6}+\frac{B}{r^{12}}\right)d\Sigma_1 d\Sigma_2, \tag{2}$$

where η_1 and η_2 denote the mean atomic surface densities of the first and the second molecules, respectively, and r is the distance between two typical surface elements $d\Sigma_1$ and $d\Sigma_2$. A and B are the attractive and the repulsive Lennard-Jones constants, respectively.

The continuum approach using the Lennard-Jones potential has been successfully employed in a number of studies to determine the van der Waals interaction energy and the force between two carbon nanostructures. Girifalco[18] determines the interaction energy between two C_{60} fullerenes, and then Girifalco *et al.*[19] extend the study to find the energy between two identical parallel carbon nanotubes of infinite length and between a carbon nanotube and a C_{60} fullerene. Further, Hodak and Girifalco[20] propose an energy formula for universal graphitic systems including the interaction of an ellipsoid inside a single-walled carbon nanotube. Ruoff and Hickman[21] consider the interaction between a spherical fullerene and a graphite sheet. Henrard *et al.*[22] use a technique similar to that of Girifalco[18] and obtain the potential for bundles of single-walled carbon nanotubes. For spherical carbon onions $C_{N_1}@C_{N_2}$ $(N_2>N_1)$, Iglesias-Groth *et al.*[23] also adopt the Lennard-Jones potential and the continuum approximation to determine the interlayer interaction. By using the formula of Iglesias-Groth *et al.*,[23] Guérin[24] obtains the interaction energy between the interlayer of carbon onions which is in excellent agreement to those obtained from discrete atom-atom summation model given by Lu and Yang.[25] Further, it is also shown by Verberck and Michel[26] that for large carbon nanotubes ($b \geqslant 7.5$ Å), the continuum approach agrees well with an atomistic model. We note that it is possible to combine both the continuum and discrete approaches to model an interaction between two nanostructures. As shown by both Verberck and Michel[26] and Hilder and Hill,[27] the single-walled carbon nanotube is modeled as a continuum, while the fullerene is assumed to retain its discrete atomic structure. Finally, we note that the validity of using the continuum approach over the discrete atom-atom model is discussed by Girifalco *et al.*[19] who point out that from a physical point of view, both discrete (e.g., molecular dynamical simulations) and continuum models make assumptions that are incorrect, and perhaps it can be argued that the continuum model is closer to reality.

To determine the interaction energy between a spherical fullerene and a carbon nanotube for a typical point on the carbon nanotube, we first perform the surface integral of the Lennard-Jones potential over the sphere. Following the work of Cox *et al.*[9,28] for a typical point on the tube, the potential energy between the C_{60} fullerene is given by

$$P = \frac{2\eta_f\pi a}{\rho}\left[\frac{A}{4}\left(\frac{1}{(\rho+a)^4}-\frac{1}{(\rho-a)^4}\right)-\frac{B}{10}\left(\frac{1}{(\rho+a)^{10}}-\frac{1}{(\rho-a)^{10}}\right)\right], \tag{3}$$

where η_f denotes the mean atomic surface density of the C_{60} molecule, a is the radius of the C_{60} fullerene which is 3.55 Å, and ρ is the distance from the center of the C_{60} molecule to the surface of the carbon nanotube. Moreover, Eq. (3) can also be rewritten as

$$P = 4\pi a^2\eta_f\left[\frac{B}{5}\left(\frac{5}{(\rho^2-a^2)^6}+\frac{80a^2}{(\rho^2-a^2)^7}+\frac{336a^4}{(\rho^2-a^2)^8}+\frac{512a^6}{(\rho^2-a^2)^9}+\frac{256a^8}{(\rho^2-a^2)^{10}}\right)-A\left(\frac{1}{(\rho^2-a^2)^3}+\frac{2a^2}{(\rho^2-a^2)^4}\right)\right]. \tag{4}$$

III. ENCAPSULATION OF C_{60} BY HEAD-ON AT AN OPEN END

The encapsulation of a C_{60} molecule into a single-walled carbon nanotube by head-on at the tube open end, as shown in Fig. 1, is determined here. We assume that the C_{60} fullerene is located on the tube axis and initially at rest. In fact, this is the model of Cox *et al.*[9] for the acceptance condition and suction energy of the C_{60} fullerene and the single-walled carbon nanotube.

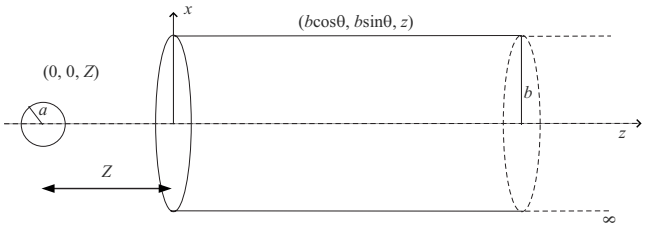

FIG. 1. C_{60} fullerene encapsulated in carbon nanotube by head-on at open end.

With reference to a rectangular Cartesian coordinate system (x,y,z) with origin located at the tube end, a typical point on the surface of the tube has the coordinates $(b\cos\theta, b\sin\theta, z)$, where b is the radius of the semi-infinite tube. Similarly, with reference to the same rectangular Cartesian coordinate system (x,y,z), the center of the C_{60} molecule has coordinates $(0,0,Z)$, where Z is the distance in the z direction which can be either positive or negative. Thus, the distance ρ between the center of the C_{60} fullerene and a typical point on the tube is given by

$$\rho^2 = b^2 + (z - Z)^2. \tag{5}$$

Using the Lennard-Jones potential function together with the continuum approximation, the total potential can be written as

$$E = b\eta_g \int_{-\pi}^{\pi} \int_{0}^{\infty} P dz d\theta,$$

where P is defined in Eq. (4), η_g represents the mean atomic surface density of the carbon nanotube, and ρ is given in Eq. (5). The integrals which need to be evaluated are all of the form

$$G_n = \int_{-\pi}^{\pi} \int_{0}^{\infty} \frac{1}{(\rho^2 - a^2)^n} dz d\theta$$

$$= \int_{-\pi}^{\pi} \int_{0}^{\infty} \frac{1}{[b^2 - a^2 + (z - Z)^2]^n} dz d\theta, \tag{6}$$

where n is a certain positive integer. It is clear that Eq. (6) is independent of θ so that we may deduce

$$G_n = 2\pi \int_{0}^{\infty} \frac{1}{[b^2 - a^2 + (z - Z)^2]^n} dz. \tag{7}$$

The details for the analytical expression of Eq. (7) are presented in Appendix A and the numerical solution is now evaluated as follows.

Using the parameter values in Table I, we show graphically in Fig. 2 the relation between the potential energy and the distance Z for the C_{60} molecule encapsulated into the (10,10), (16,16), and (20,20) carbon nanotubes by head-on. The energetically most favorable location for the C_{60} fullerene is inside the tube, in the positive direction of Z, for all three cases, which is shown in Fig. 2. Furthermore, the binding energies which are the energies required to separate the two bodies are 3.222, 0.326, and 0.109 eV for the (10,10), (16,16), and (20,20) carbon nanotubes, respectively.

TABLE I. Values of constants [* denotes the data taken from Girifalco *et al.* (Ref. 19)].

Radius of C_{60} (a)	3.55 Å
Radius of (10,10) (b)	6.784 Å
Radius of (16,16) (b)	10.846 Å
Radius of (20,20) (b)	13.557 Å
Attractive constant-C_{60}-graphene (A)	17.4 eV Å^{6*}
Repulsive constant-C_{60}-graphene (B)	29.0×10^3 eV Å^{12*}
Mean surface density of C_{60} (η_f) $[60/(4\pi a^2)]$	0.3789 Å^{-2}
Mean surface density of carbon nanotube (η_g) $[4\sqrt{3}/(9\sigma^2)]$	0.3812 Å^{-2}
C-C bond length (σ)	1.42 Å

We observe that the lowest potential energy occurs for the case of the (10,10) tube, since the preferred location of the C_{60} molecule is on the tube axis.[19] As a result, offset locations from the tube axis for the (16,16) and (20,20) tubes are required to give rise to the most stable configurations and these details can be found in Girifalco *et al.*[19] and Cox *et al.*[28]

IV. ENCAPSULATION OF C_{60} AROUND THE EDGE AT AN OPEN END

In this section, the energy for a C_{60} molecule encapsulated into a carbon nanotube by entering the tube around the tube edge at the open end is investigated. With reference to the same rectangular Cartesian coordinate system (x,y,z), a typical point on the surface of the tube has the coordinates $(b\cos\theta, b\sin\theta, z)$, where b is the radius of the semi-infinite tube. Similarly, with reference to the rectangular Cartesian coordinate system (x,y,z), the center of the C_{60} molecule has coordinates $(x,0,Z)$, where Z is the distance in the z direction which can be either positive or negative. The distance Z and the coordinate x can also be described in terms of an angle ϕ and the distance r in the radial direction which are $Z = r\cos\phi$ and $x = r\sin\phi + b$, as illustrated in Fig. 3.

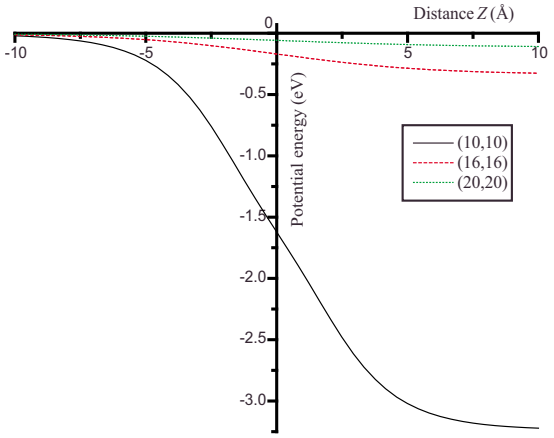

FIG. 2. (Color online) Energy profile for C_{60} encapsulated by head-on at open end.

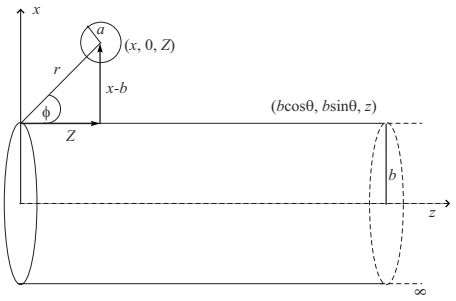

FIG. 3. C_{60} fullerene encapsulated in carbon nanotube around edge at open end.

Thus, the distance ρ between the center of the C_{60} fullerene and a typical point on the tube is given by

$$\rho^2 = (b\cos\theta - x)^2 + b^2\sin^2\theta + (z-Z)^2$$
$$= (b-x)^2 + 4bx\sin^2(\theta/2) + (z-Z)^2. \quad (8)$$

The total potential energy is obtained by integrating P, which is defined by Eq. (4), over the tube length and the angle θ. Thus, there is one form of the integral which needs to be evaluated and we may deduce

$$H_n = \int_{-\pi}^{\pi}\int_0^{\infty} \frac{1}{(\rho^2 - a^2)^n} dz d\theta, \quad (9)$$

where ρ is given by Eq. (8). Further, there are three possible expressions for Eq. (9) and these details are presented in Appendix B. Although the analytical expressions for Eq. (9) are clearly complicated, numerical values may be readily evaluated using the algebraic computer package MAPLE. We note that the total potential energy in terms of the distance r and the angle ϕ can be obtained by replacing $Z=r\cos\phi$ and $x=r\sin\phi+b$.

To confirm our results, the numerical evaluation for the encapsulation of the C_{60} molecule around the edge at the tube end is determined using both the polar coordinate system and the Cartesian coordinate system expressions for the integrals. In terms of the polar coordinate system, we show numerically the relation between the binding energy and the groove site for different angles ϕ, as presented in Table II. We observe that the lowest binding energy occurs at $\phi \approx 165°$ for all three cases due to the edge effect. Consequently, this value of ϕ is the critical value whether or not the C_{60} molecule is encapsulated into the tube. The terminology "groove site," refers to the cross-sectional location adopted by the C_{60} fullerene in the carbon nanotube, and it is defined as the distance between the tube edge and the center of the fullerene at equilibrium. The groove sites are obtained as 6.775, 6.540, and 6.550 Å for $\phi=270°$ and for each of the (10,10), (16,16), and (20,20) tubes, respectively. These values are equivalent to 0.009, 4.306, and 7.007 Å, respectively, away from the tube axis to the center of the C_{60} fullerene in the x direction, which are in agreement with the work of Cox *et al.*[28]

In terms of the Cartesian coordinate system, the potential energy of the system depends on both distances in the x and z directions. We show graphically an example of the potential energy versus the distance Z for the encapsulation of the C_{60} fullerene into the (10,10) tube. Primarily, our interest is in the positive z direction where the C_{60} molecule is located

TABLE II. Numerical values for binding energy (BE) in eV and the groove site (GS) in Å for a C_{60} fullerene encapsulated in a carbon nanotube around the tube edge at the open end for different angles ϕ.

	(10,10)		(16,16)		(20,20)	
	BE	GS	BE	GS	BE	GS
15°	0.53424	25.16055	0.58315	25.14903	0.60398	25.14903
30°	0.53026	13.01349	0.57883	13.00486	0.59953	13.00486
45°	0.51050	9.18529	0.55756	9.20351	0.57737	9.18603
60°	0.45467	7.53991	0.49675	7.56151	0.51479	7.54922
75°	0.35970	6.77549	0.39343	6.79463	0.40775	6.81484
90°	0.26722	6.47536	0.29169	6.51166	0.30211	6.51166
105°	0.20322	6.32529	0.22146	6.36167	0.22892	6.35916
120°	0.16640	6.30654	0.17929	6.32301	0.18476	6.32103
135°	0.14647	6.26761	0.15413	6.21275	0.15967	6.28291
150°	0.13894	6.26761	0.14378	6.21275	0.14722	6.28291
165°	0.14169	6.26761	0.14250	6.21275	0.14412	6.28291
180°	0.15563	6.26761	0.14998	6.21275	0.14929	6.28291
195°	0.18511	6.26761	0.16666	6.21275	0.16318	6.28291
210°	0.24079	6.30654	0.19779	6.30216	0.18779	6.28291
225°	0.34809	6.34427	0.24633	6.30216	0.22694	6.32103
240°	0.56623	6.44215	0.32206	6.34055	0.28746	6.32103
255°	1.01175	6.66655	0.43751	6.42551	0.38012	6.40225
270°	1.62119	6.77519	0.60665	6.53999	0.51827	6.55048

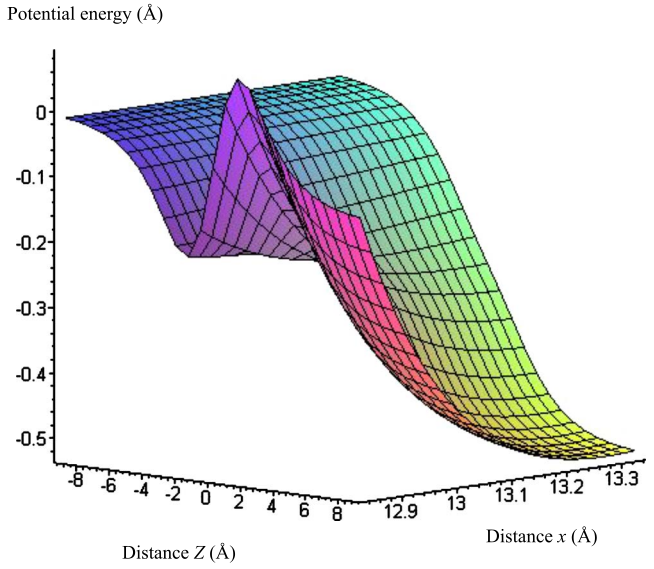

FIG. 4. (Color online) Energy profile for C_{60} encapsulated into a (10,10) tube.

above the tube. As shown in Fig. 4, the C_{60} fullerene will not be encapsulated into the tube if its location is far away from the edge of the tube. This is because of the lower energy level at that position and the high energy peak near the tube end. However, a nanopeapod might be formed if an initial energy is given for the C_{60} molecule to overcome the energy barrier. The C_{60} fullerene has a greater probability of encapsulation around the tube edge if it is initiated from rest closer to the tube edge. If the value of x is greater than 13.034 Å, the C_{60} fullerene has no chance of being sucked into the carbon nanotube since the global minimum energy position is located further along the tube in the positive z direction. We note that for the C_{60} molecule which can overcome the energy barrier and located in the negative z direction, the analysis for the suction by head-on applies for the encapsulation.

V. ENCAPSULATION OF C_{60} AT A DEFECT OPENING ON THE TUBE WALL

In this section, we determine the potential energy for a C_{60} fullerene encapsulated into a carbon nanotube at a defect opening on the tube wall which is centrally located midway along the tube length. Since the Lennard-Jones potential is only effective at short range, the carbon nanotube is assumed to be infinite in length. From Eq. (2), the total potential energy of the system is obtained by subtracting the total energy for the C_{60} fullerene interacting with the defect pad from the total potential energy for the C_{60} fullerene interacting with the infinite carbon nanotube, as illustrated in Fig. 5.

Again, with reference to the rectangular Cartesian coordinate system (x,y,z), a typical point on the surface of the tube has the coordinates $(b\cos\theta, b\sin\theta, z)$, where b is the radius of the infinite tube. Similarly, with reference to the rectangular Cartesian coordinate system (x,y,z) with origin located at the center of the tube, the center of the C_{60} molecule is

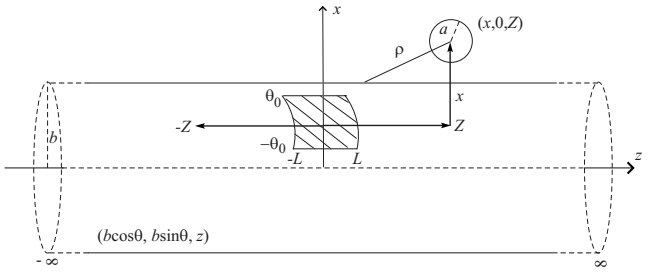

FIG. 5. C_{60} fullerene encapsulated in carbon nanotube at defect opening on the tube wall.

assumed to have coordinates $(x,0,Z)$, where Z is the distance in the z direction which can be either positive or negative. Thus, the distance ρ between the center of the C_{60} fullerene and a typical point on the tube is given by

$$\rho^2 = (b\cos\theta - x)^2 + b^2\sin^2\theta + (z-Z)^2$$
$$= (b-x)^2 + 4bx\sin^2(\theta/2) + (z-Z)^2. \quad (10)$$

Thus, the total potential energy for the entire tube interacting with the C_{60} fullerene is given by

$$E_{tube} = b\eta_g \int_{-\pi}^{\pi}\int_{-\infty}^{\infty} P dz d\theta, \quad (11)$$

where η_g denotes the mean atomic surface density of the carbon nanotube, P is defined by Eq. (4), and ρ is given in Eq. (10). The defect pad is assumed occupied in the region $Z \in (-L,L)$ and $\theta \in (-\theta_0,\theta_0)$ so that the interacting energy between the C_{60} molecule and the defect pad is given by

$$E_{pad} = b\eta_g \int_{-\theta_0}^{\theta_0}\int_{-L}^{L} P dz d\theta, \quad (12)$$

where ρ is again given by Eq. (10). Thus, the total potential energy for the C_{60} fullerene encapsulated in the carbon nanotube at the defect opening on the tube wall is obtained from

$$E = b\eta_g\left(\int_{-\pi}^{\pi}\int_{-\infty}^{\infty} P dz d\theta - \int_{-\theta_0}^{\theta_0}\int_{-L}^{L} P dz d\theta\right). \quad (13)$$

By precisely the same analytical method as shown in Sec. IV, we separately determine Eqs. (11) and (12) and numerically calculate the total potential energy (13) for the system.

Numerical solutions for the C_{60} encapsulated into the (10,10), (16,16), and (20,20) carbon nanotubes at the defect opening on the tube wall are determined here. The defect pad is arbitrarily chosen to be a square such that the length L is the radius a of the C_{60} fullerene plus the equilibrium interspacing between the C_{60} fullerene and the graphene which is 3.25 Å.[19] Using the arc length formula $s=b\theta$, we adopt the limit of the integration θ_0 to be determined from $L=b\theta_0$. We note that varying θ_0 has only a minor effect on the energy profile and that the overall properties of the system remain the same when L is greater than the critical value 6.8 Å.

We examine the relation between the potential energy and the distance Z for the different values of x, which is the interspacing between the C_{60} molecule and the tube wall,

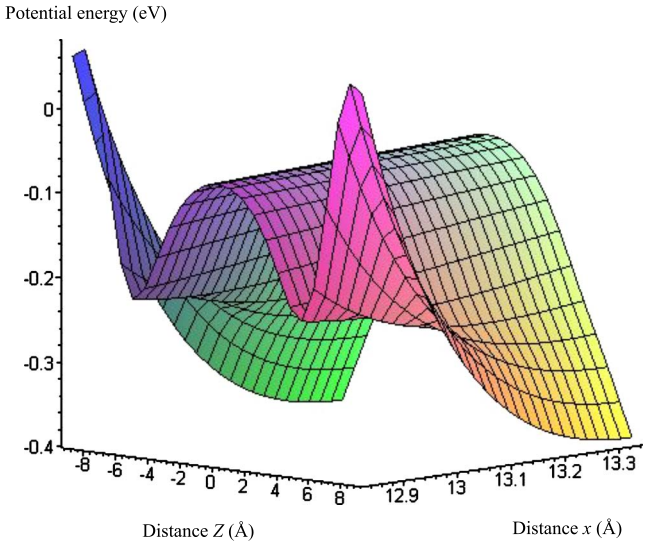

FIG. 6. (Color online) Potential energy profile along the (10,10) tube.

and we obtain similar behavior for all cases. An example for the energy profile for the interacting of the C_{60} molecule and the (10,10) tube is shown in Fig. 6. In terms of the binding energy, we concern such energy at both edges of the defect pad because of the point force singularity effected from the edges. In this case, we obtain an approximate value at 0.225 eV from both edges of the defect pad. Using the Boltzmann formula $3kT/2$ for kinetic energy, this corresponds to a temperature of approximately 1972 K, and therefore to achieve the same effect at room temperature requires an energy of 0.039 eV. We also observe two potential energy peaks near the edges of the defect pad for $x \leqslant 13.034$ Å so that if the C_{60} molecule is located outside the region of the pad, an initial energy is required for the C_{60} fullerene to be absorbed into the nanotube. However, the C_{60} molecule is spontaneously sucked in through the defect opening when its position is directly above the defect. Furthermore, if the value of x is greater than 13.034 Å, the global minimum energy position is always located outside the region of the pad along the tube in the z position. Subsequently, the C_{60} fullerene will not be adsorbed through the pad and a nanopeapod cannot be formed.

VI. SUMMARY

This paper considers three suction site scenarios for a C_{60} molecule entering a carbon nanotube, which are (i) by head-on at the tube open end, (ii) around a tube edge at the tube open end, and (iii) at a defect opening on the tube wall. The C_{60} fullerene is assumed to be initially at rest prior to entering into the three specific carbon nanotubes (10,10), (16,16), and (20,20) in a vacuum environment. We employ the Lennard-Jones potential function and the continuum approximation, and double surface integrals are performed to determine the potential energy which may be expressed in terms of the hypergeometric function. Due to the complicated analytical expressions, numerical evaluations are performed by using the algebraic computer package MAPLE.

The binding energies for the three encapsulation mechanisms are compared and it is found that the C_{60} molecule is most likely to enter through the carbon nanotube by the head-on configuration. This is because of the overall attractive force arising from the entire tube, and this mechanism avoids the point force singularity acting at the tube edge. Absorption at a defect is the second most likely mechanism to form the nanopeapod. There is an effect from the edges of the defect, but when the C_{60} fullerene is directly above the defect, it is a straightforward matter for the C_{60} fullerene to be sucked into the tube. The least feasible mechanism to encapsulate the C_{60} fullerene is entering around the edge of the tube open end, since the C_{60} molecule must overcome strong repulsive forces at the tube end and change the moving direction to enter into the tube. As a result, the quantitative investigation in this study is in agreement with previous studies such as those by Ulbricht and Hertel[14] and Ulbricht *et al.*,[16] but our predictions contradict those of Berber *et al.*[15]

ACKNOWLEDGMENTS

The authors are grateful to the Australian Research Council for support through the Discovery Project Scheme. They are also especially grateful to their colleagues Barry Cox and Tamsyn Hilder for many helpful comments and discussions on this work.

APPENDIX A: EVALUATION OF INTEGRAL (7)

Equation (7) is determined here. First, we define the integral G_n^* which can be written as

$$G_n^* = \int_0^\infty \frac{dz}{[b^2 - a^2 + (z-Z)^2]^n}.$$

On letting $\lambda^2 = b^2 - a^2$ and making $x = z - Z$, we may deduce

$$G_n^* = \int_{-Z}^\infty \frac{dx}{(\lambda^2 + x^2)^n},$$

where n is a certain positive integer. We are led to make the substitution $x = \lambda \tan\psi$ and we may deduce

$$G_n^* = \int_{-\tan^{-1}(Z/\lambda)}^{\pi/2} \frac{\lambda \sec^2\psi}{\lambda^{2n}\sec^{2n}\psi} d\psi = \frac{1}{\lambda^{2n-1}} \int_{-\tan^{-1}(Z/\lambda)}^{\pi/2} \cos^{2(n-1)}\psi d\psi. \quad \text{(A1)}$$

The evaluation for Eq. (A1) can be found in Gradshteyn and Ryzhik[29] (p. 149, No. 2.513 3) from which we may deduce

$$\int \cos^{2(n-1)}\psi d\psi = \frac{1}{2^{2(n-1)}}\left[\binom{2(n-1)}{(n-1)}\psi + \sum_{k=0}^{n-2}\binom{2(n-1)}{k}\frac{\sin[(2n-2k-2)\psi]}{(n-k-1)}\right], \quad \text{(A2)}$$

where $\binom{n}{m}$ is the binomial coefficient. By evaluating Eq. (A2)

at $\psi=\pi/2$ and $\psi=-\tan^{-1}(Z/\lambda)$, an analytical expression for G_n^* may be obtained.

APPENDIX B: EVALUATION OF INTEGRAL (9)

In this appendix, we evaluate integral (9) where $\rho^2=(b-x)^2+4bx\sin(\theta/2)+(z-Z)^2$. On letting $\lambda^2=(b-x)^2+4bx\sin^2(\theta/2)-a^2$, we obtain

$$H_n=\int_{-\pi}^{\pi}\int_0^{\infty}\frac{1}{[\lambda^2+(z-Z)^2]^n}dzd\theta,$$

where n is a certain positive integer. On making the substitution $u=z-Z$, we may deduce

$$H_n=\int_{-\pi}^{\pi}\int_{-Z}^{\infty}\frac{1}{(\lambda^2+u^2)^n}dud\theta$$

$$=\int_{-\pi}^{\pi}\int_{-\tan^{-1}(Z/\lambda)}^{\pi/2}\frac{\lambda\sec^2\psi}{\lambda^{2n}\sec^{2n}\psi}d\psi d\theta,$$

where the final line is obtained by substituting $x=\lambda\tan\psi$. Finally, we have

$$H_n=\frac{1}{\lambda^{2n-1}}\int_{-\pi}^{\pi}\int_{-\tan^{-1}(Z/\lambda)}^{\pi/2}\cos^{2(n-1)}\psi d\psi d\theta.$$

By using the formula given by Eq. (A2) and evaluating the above equation at $\psi=\pi/2$ and $\psi=-\tan^{-1}(Z/\lambda)$, there are three forms for the integral for $\theta\in(0,\pi/2)$ which need to be determined and they are given by

$$I_s=\int_0^{\pi/2}\frac{dv}{\lambda^s},\quad J_{s,t}=\int_0^{\pi/2}\frac{dv}{\lambda^t(\lambda^2+Z^2)^s},$$

$$K_s=\int_0^{\pi/2}\frac{1}{\lambda^s}\tan^{-1}\left(\frac{Z}{\lambda}\right)dv, \tag{B1}$$

where λ is defined by $\lambda^2=(b-x)^2+4bx\sin^2(v/2)-a^2$. The integrals in Eq. (B1) are evaluated in Baowan *et al.*[30] and yield

$$I_s=\frac{\pi}{2(b+x)^s}F\left(\frac{s}{2},\frac{1}{2};1;\frac{4bx}{(b+x)^2}\right),$$

$$J_{s,t}=\frac{\pi}{2(b+x)^t[(b+x)^2+Z^2]^s}\sum_{i=0}^{\infty}\frac{(1/2)_i(t/2)_i}{(i!)^2}F\left(\frac{1}{2}+i,s;1+i;\frac{4bx}{(b+x)^2+Z^2}\right)\left[\frac{4bx}{(b+x)^2}\right]^i,$$

$$K_s=\frac{\pi}{2(b+x)^s}\sum_{k=0}^{\infty}\sum_{i=0}^{\infty}\frac{Z^{2k+1}(2k)!}{2^{2k}(k!)^2(2k+1)[(b+x)^2+Z^2]^{k+1/2}}\frac{(1/2)_i(s/2)_i}{(i!)^2}F\left(\frac{1}{2}+i,\frac{1}{2}+k;1+i;\frac{4bx}{(b+x)^2+Z^2}\right)\left[\frac{4bx}{(b+x)^2}\right]^i,$$

where $F(a,b;c;z)$ denotes the standard hypergeometric function.

[1] M. S. Dresselhaus, G. Dresselhaus, and P. C. Eklund, *Science of Fullerenes and Carbon Nanotubes*, 1st ed. (Academic, California, 1995).
[2] P. J. F. Harris, *Carbon Nanotubes and Related Structures*, 1st ed. (Cambridge University Press, Cambridge, UK, 2003).
[3] B. W. Smith, M. Monthioux, and D. E. Luzzi, Nature (London) **396**, 323 (1998).
[4] B. W. Smith and D. E. Luzzi, Chem. Phys. Lett. **321**, 169 (2000).
[5] M. Otani, S. Okada, and A. Oshiyama, Phys. Rev. B **68**, 125424 (2003).
[6] D. Qian, W. K. Liu, and R. S. Ruoff, J. Phys. Chem. B **105**, 10753 (2001).
[7] S. Okada, S. Saito, and A. Oshiyama, Phys. Rev. Lett. **86**, 3835 (2001).
[8] M. Hodak and L. A. Girifalco, Phys. Rev. B **68**, 085405 (2003).
[9] B. J. Cox, N. Thamwattana, and J. M. Hill, Proc. R. Soc. London, Ser. A **463**, 461 (2007).
[10] A. Rochefort and CERCA-Groupe Nanostructures, Phys. Rev. B **67**, 115401 (2003).
[11] E. González Noya, D. Srivastava, L. A. Chernozatonskii, and M. Menon, Phys. Rev. B **70**, 115416 (2004).
[12] M. Yoon, S. Berber, and D. Tomanek, Phys. Rev. B **71**, 155406 (2005).
[13] K. H. Michel, B. Verberck, and A. V. Nikolaev, Phys. Rev. Lett. **95**, 185506 (2005).
[14] H. Ulbricht and T. Hertel, J. Phys. Chem. B **107**, 14185 (2003).
[15] S. Berber, Y.-K. Kwon, and D. Tomanek, Phys. Rev. Lett. **88**, 185502 (2002).
[16] H. Ulbricht, G. Moos, and T. Hertel, Phys. Rev. Lett. **90**, 095501 (2003).
[17] M. Hodak and L. A. Girifalco, Phys. Rev. B **67**, 075419 (2003).
[18] L. A. Girifalco, J. Phys. Chem. **96**, 858 (1992).
[19] L. A. Girifalco, M. Hodak, and R. S. Lee, Phys. Rev. B **62**, 13104 (2000).

[20] M. Hodak and L. A. Girifalco, Chem. Phys. Lett. **350**, 405 (2001).
[21] R. S. Ruoff and A. P. Hickman, J. Phys. Chem. **97**, 2494 (1993).
[22] L. Henrard, E. Hernández, P. Bernier, and A. Rubio, Phys. Rev. B **60**, R8521 (1999).
[23] S. Iglesias-Groth, J. Breton, and C. Girardet, Chem. Phys. Lett. **264**, 351 (1997).
[24] H. Guérin, J. Phys. B **30**, L481 (1997).
[25] J. P. Lu and W. Yang, Phys. Rev. B **49**, 11421 (1994).
[26] B. Verberck and K. H. Michel, Phys. Rev. B **74**, 045421 (2006).
[27] T. A. Hilder and J. M. Hill, J. Phys. A **40**, 3851 (2007).
[28] B. J. Cox, N. Thamwattana, and J. M. Hill, Proc. R. Soc. London, Ser. A **463**, 477 (2007).
[29] I. S. Gradshteyn and I. M. Ryzhik, *Table of Integrals, Series, and Products*, 6th ed. (Academic, New York, 2000).
[30] D. Baowan, N. Thamwattana, and J. M. Hill (to be published).